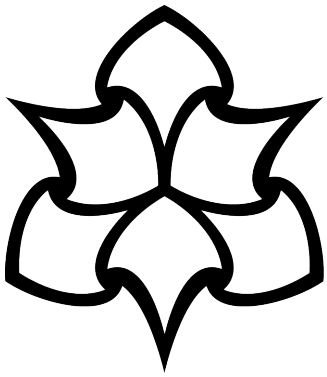

Available online at www.sciencedirect.com

ScienceDirect

Procedia Engineering 199 (2017) 423–428

Procedia Engineering

www.elsevier.com/locate/procedia

X International Conference on Structural Dynamics, EURODYN 2017

Output-only full-field modal testing

Yen-Hao Chang[a,b], Weizhuo Wang[c], Eann A. Patterson[a], Jen-Yuan Chang[b], John E. Mottershead[a,d*]

[a] *Department of Mechanical, Aerospace and Materials Engineering, University of Liverpool, UK*
[b] *Department of Power Mechanical Engineering, National Tsing Hua University, Taiwan*
[c] *School of Engineering, Manchester Metropolitan University, UK*
[d] *Institute for Risk and Uncertainty, University of Liverpool, UK*

Abstract

Operational modal analysis has become the focus of much research attention in the last two decades. Instead of an artificial force, the ambient excitation is considered as white-noise input to the structure and modal properties are calculated only from measured responses. In terms of the measurement technique, full-field optical methods, for example: electronic speckle pattern interferometry and digital image correlation have become popular and there is now much interest in applying these methods in structural dynamics. In this case the generated data is a full displacement map of the object, therefore there is no necessity to select specific measurement locations in order to visualise the deformation. However, there are generally large volumes of data to be processed, which makes the computation expensive and time-consuming, especially for engineering structures with large surface areas. Thanks to image decomposition techniques, huge amounts of data can be compressed into tens of *shape descriptors* with acceptably small distortion. In this paper, operational modal analysis and full-field methods are combined together, and the analysis is done in the shape descriptor domain to reduce the required computation time. Simulated responses from a finite element model of a clamped plate (under random excitation) serve to illustrate the methodology. Several different operational modal analysis methods are applied to analyse the data, and results are provided for purposes of comparison.

Peer-review under responsibility of the organizing committee of EURODYN 2017.

Keywords: Operational modal analysis; Full-field measurement; Image decomposition.

*Corresponding author: John E. Mottershead, Department of Mechanical, Aerospace and Materials Engineering, University of Liverpool, Harrison-Hughes Building, The Quadrangle, Liverpool L69 3GH, UK.
E-mail address: j.e.mottershead@liv.ac.uk (J. E. Mottershead).

1877-7058
Peer-review under responsibility of the organizing committee of EURODYN 2017.
10.1016/j.proeng.2017.09.137

1. Introduction

Experimental modal analysis (EMA) [1] is a tool that allows engineers to understand the dynamic performance of structures from vibration tests. It is regularly used for the verification and validation of mathematical (e.g. finite element) models used in engineering design. When in-situ, boundary conditions and loads might be quite different from the ideal conditions assumed in design, and for that reason it is often necessary to carry out modal tests under operating conditions. The use of artificial excitation (e.g. using electromagnetic shakers) is often impractical as well as involving an unnecessary expense. Instead, modern techniques are now available that make use of the ambient excitation due for example to wind loads or passing traffic. Such methods, often referred to as operational modal analysis (OMA), inevitably make assumptions on the character of the noise, the principal assumption being that it can be treated as Gaussian white noise. A tutorial review of OMA techniques is given by Magalhaes and Cunha [2].

The use of optical methods, such as digital image correlation (DIC) [3], in vibration testing has become a prominent research topic in recent years and offers potentially significant advantages over traditional accelerometer-based measurements. These include measurement across the complete field of view entirely without added-mass effects, which can be significant especially for close modes when measurement are made with accelerometers. Wang and Mottershead [4] proposed the use of image decomposition to reduce the large volume of pixelated output data to an acceptably small volume of features, or shape descriptors (SD), for efficient processing of full-field measurements.

The purpose of this paper is to demonstrate the application of full-field operational modal testing using outputs in the SD domain. Sections 2 and 3 provide brief overviews of OMA and SD techniques. This is followed in Section 4 by a numerical example to illustrate the performance of several OMA/SD techniques. Finally the work is concluded with statements on effectiveness of the proposed combined approach.

2. Brief overview of operational modal analysis

There are now numerous OMA methods developed from the well-established EMA theories. One of the earliest was the Ibrahim time domain method [5], originally used to calculate the modal properties from free responses. In order to create the required free decay signal for the processing, the covariance or random decrement techniques were applied to measured data. The resulting signals were proven to have the characteristic of free response [6].

The well-known stochastic subspace identification (SSI) method was described in detail by Peeters and De Roeck [7]. Using time series methods and the discrete stochastic state-space, the data were arranged in a Hankel matrix divided into two parts corresponding to shifted ‘past’ and the ‘future’ measurements referred to the i^{th} time increment. In theory the Hankel matrix should have an infinite number of rows, whereas in practice it is assumed that the data is sufficiently plentiful to obtain modal estimates of sufficient accuracy. The covariance-driven SSI makes use of the properties of the Toeplitz matrix of covariance terms, whereas the data-driven SSI is based on QR factorization of the block Hankel matrix to project the row space of future outputs on the row space of past reference outputs. Determination of the state-space system matrices is achieved (a) by the covariance-driven SSI, using singular value decomposition of the Toepliz matrix, which leads to the determination of the observabilty and controllability matrices; and (b) by the data-driven SSI, which requires a further projection at time increment i+1. A stabilization diagram may be drawn in order to visually identify the stable modes.

The frequency-domain decomposition (FDD) method [8] applies singular value decomposition (SVD) to the spectrum matrix of auto- and cross-spectra, thereby producing the maximum singular value spectrum for the extraction of modes by peak-picking (PP). An alternative method using transmissibility [9, 10] may also applied to establish frequency spectrum by SVD, based on the principle that the difference between two transmissibility functions, with the same output but different inputs, vanishes at the poles of the system.

The poly-reference least square complex frequency-domain (P-LSCF) method [11], known commercially as *PolyMax*, is based upon the minimization of a cost function, the difference between the measured transfer function and the theoretical right matrix fraction model expressed in terms of polynomial matrices. Natural frequencies, damping ratios and mode shapes may be determined from state-space system matrices via the estimated polynomial matrices.

An early example of the frequency-domain Bayesian approach to OMA is described by Yuen and Katafygiotis [12], later modified to improve the computation efficiency by Au [13]. The method is based upon the application of Bayes rule with the posterior estimate of the PDF of modal parameters given (within a constant of proportionality)

by the product of the likelihood function and the prior, the latter given by a constant (uninformative prior) in cases when no prior information is available.

3. Brief overview of image decomposition and shape descriptors (SD)

Image decomposition encompasses a class of techniques already well-established in other disciplines such as forensics and medicine, but is less well known in in the processing of engineering images. The general purpose is the compression of digital images occupying large volumes of storage space. Significant amounts of this data are effectively redundant when the image under consideration contains shapes of reasonably low spatial frequency, such as low frequency vibration mode shapes. It is this redundancy that is eliminated by image processing using SDs. Thus raw images containing typically hundreds of thousands of data points may be reduced to a few tens (or hundreds) of SD terms with acceptably small loss of fidelity. The truncation of higher order spatial-frequency SD terms has the beneficial effect of removing measurement noise.

The procedure consists of the selection (or development) of a system of kernel functions, which for reasons of efficiency are usually chosen to be orthogonal [14]. The classical orthogonal polynomials, typically the Zernike and Tchebichef polynomials are orthogonal upon circular and rectangular bases respectively and are immediately applicable to the processing of displacement (and strain) images obtained from discs and rectangular panels in engineering [15, 16].

However, in the general case the system of kernel functions must be flexible enough for engineering structures, which come in an almost endless variety of shapes and sizes, to be included. Then the procedure is to begin with a system of monomials, which must be tailored to the irregular outline of the surface upon which measurements are to be taken – if there are holes or internal cut-outs, then these should also be treated as boundaries to be tailored. For curved (non-flat) surfaces it is necessary to apply conformal mapping so that the measured image is made planar. The application of Gram-Schmidt orthonormalisation to the tailored monomials then results in the required kernel functions. The SDs, in this case known as adaptive geometric moment descriptors (AGMD) [4], are the coefficients of the kernel functions required to reproduce the measured data. Wang and Mottershead [17] used AGMDs in the EMA of a Fiat Punto car bonnet liner. Truncation of the AGMDs to retain only those that made the most significant contributions to the mode shapes resulted in the compression of 14,158 DIC data points to 20 shape descriptors without any significant loss of accuracy in the displacement fields of the first eleven mode shapes. Modal analysis in the shape feature domain results in mode-shape vectors with each term representing a SD (rather than the displacement at a discrete spatial location).

4. Numerical Example

In order to demonstrate how the proposed method works, a set of time domain displacement data generated from a clamped rectangular steel plate serve as the object of dynamic analysis. The simulated data was produced using the finite element code ABAQUS. The details are listed in Table 1.

Table 1. Simulation details.

Property	Description
Material	A36 Steel: Young's modulus: 200GPa Poisson ratio: 0.26 Density: 7850 Kg/m^3 Isotropic
Dimension	Width: 1 m Height: 0.5 m Thickness: 0.003 m
Section	Solid, Homogeneous
Mesh	Width × Height × Thickness: 100 × 50 × 3 elements
Element type	3D brick element, 8 nodes
Boundary condition	Both right and left sides are 6 DOFs fixed
Load	Location: 0.4m x 0.05m from the top left corner Excitation: Zero-mean Gaussian white noise Standard deviation: 13.2 N (maximum amplitude: 50 N)
Sampling frequency	1000 Hz
Number of steps	2500 (2.5 sec)
Output	5151 out-of-plane displacement recordings

4.1 Shape descriptors and vibration shape reconstruction

Monomials with subsequent orthonormalisation by the Gram-Schmidt process are chosen as SDs, the first 24 being used for shape decomposition. The raw data with a storage requirement of 196 megabyte (MB) is compressed to roughly 1.31 MB including the SDs and kernels. All SD signals are presented in Fig. 1. The correlation coefficient of reconstructed shapes relative to the measured displacement shapes are plotted against time in Fig. 2. The resulting average correlation of all instants is 0.988, which means the reconstructed shapes can represent the measured ones with acceptably slight distortion. An example of comparison of measured deflected shape and reconstructed one is provided in Fig. 3. The corresponding bar graph of SDs at the instant of 1250 milliseconds is given in Fig. 4.

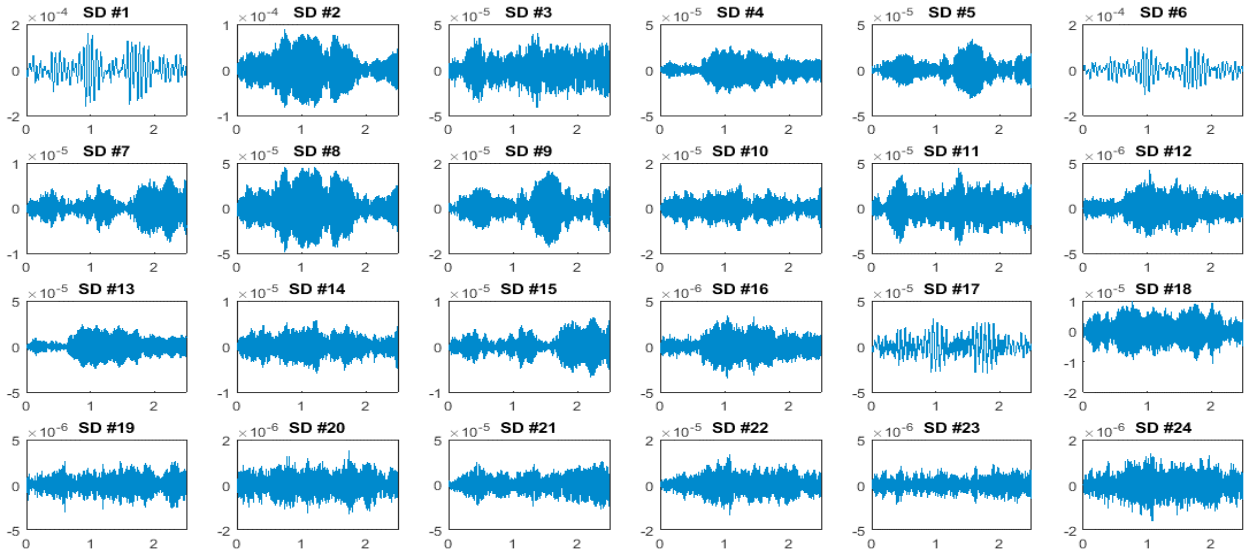

Fig. 1. The SD signals. The vertical axes represent the amplitude in metres and the horizontal axes the sampling time in seconds.

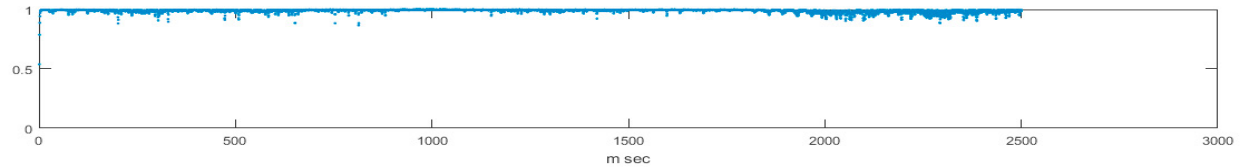

Fig. 2. The correlation coefficients of instantaneous shapes reconstructed by 24 SDs – the horizontal axis denotes time in seconds.

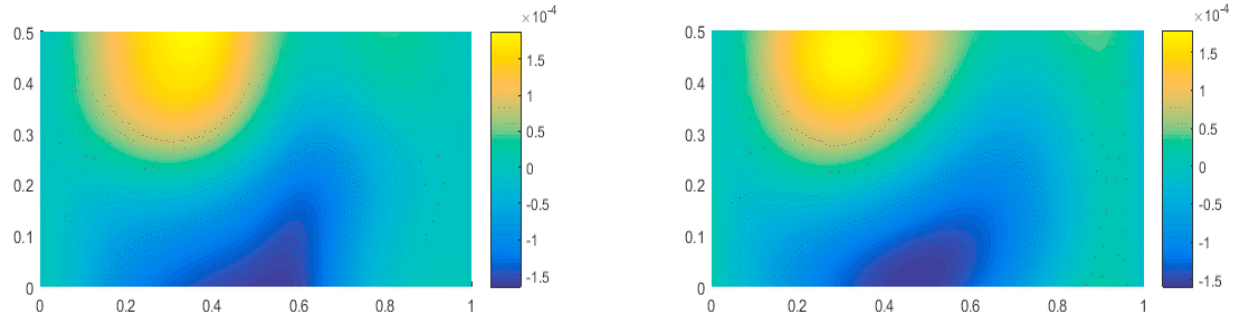

Fig. 3. The plot on the left is the deflected shape at 1250 milliseconds, and the right is the reconstructed shape using 24 SD terms (correlation coefficient: 0.9926). The color bars represent displacement in metres.

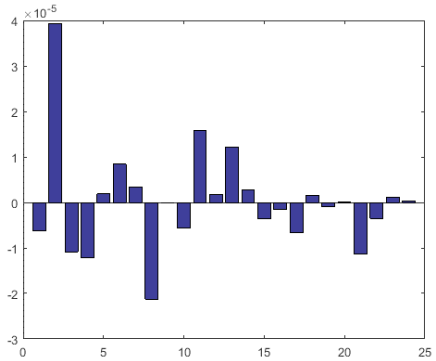

Fig. 4. SD bar graph at 1250 milliseconds. The vertical axis represents the amplitude in metres, and the horizontal axis denotes the SD number.

4.2 Natural frequencies and mode shapes

Natural frequency differences between FEA and those obtained by each of the OMA methods are presented as a percentage of the FEA results in Table 2.

Table 2. The result of frequencies in Hz.

Mode number	1	2	3	4	5	6	7	8
FEA	15.146	41.797	59.181	82.018	118.55	131.19	135.68	183.15
FDD	15.63	41.99	59.08	81.54	117.19	128.91	133.3	177.25
Difference	3.20	0.46	0.17	0.58	1.15	1.74	1.75	3.22
Bayesian	14.84	41.79	59.55	81.47	116.9	128.91	133.12	177.63
Difference	2.02	0.02	0.62	0.67	1.39	1.74	1.89	3.01
P-LSCF	18.08	43.335	60.9	83.21	118.69	130.49	134.37	no
Difference	19.37	3.68	2.90	1.45	0.12	0.53	0.97	no
SSI-COV	15.29	41.74	59.27	81.59	117.05	129.25	133.26	177.74
Difference	0.95	0.14	0.15	0.52	1.27	1.48	1.78	2.95
SSI-DATA	15.17	41.72	59.26	81.59	117.04	129.23	133.25	177.72
Difference	0.16	0.18	0.13	0.52	1.27	1.49	1.79	2.96

The first eight mode shapes identified by each method are compared with those computed by FEA, and the corresponding MAC maps are provided in Fig. 5.

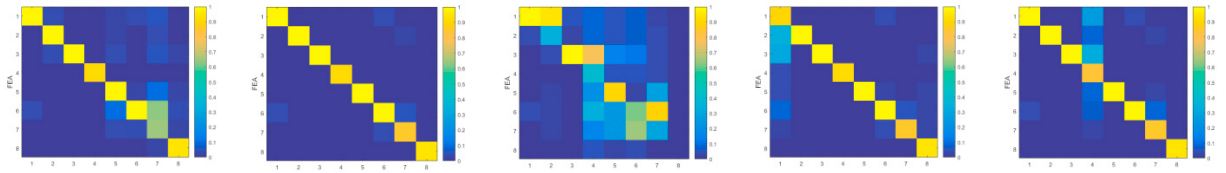

(a) FDD (b) Bayesian (c) P-LSCF (d) SSI-COV (e) SSI-Data

Fig. 5. MAC maps of different methods.

5. Discussion and conclusions

In the simulation, a continuous rectangular plate was chosen as the object for simplicity of demonstration. With the number of data points at circa 5000, it is not possible to process it with a personal computer having limited computational memory. By using SD compression, the large volume of data is reduced to only 24 SDs and kernels, and the reconstructed shape data during measurement, as shown in Fig. 2, has an average correlation coefficient of 0.988, which means that the SD reconstructed signals represent the original ones with very high levels of accuracy.

From Table 2, most of the frequency differences between each OMA method and FEA are within 4%. However, this is not the case for those calculated by P-LSCF method, which involves two steps of ill-conditioned inversions in the computation and appears to be sensitive to the level of noise excitation. Mode shapes are similarly affected as can be seen in the MAC values in Fig. 5. The reason why the MAC value of 7^{th} mode shape in FDD method is lower than 0.8 is thought to be due to peak picking (PP). This paper demonstrates the combination of SD technique and OMA methods for the identification of modal properties. Further work is planned to demonstrate the effectiveness of full-field OMA experimentally.

Acknowlegdement

Yen-Hao Chang wishes to acknowledge the support provided by a University of Liverpool / NTHU scholarship through the dual PhD programme.

References

[1] D. J. Ewins, Modal Testing: Theory and Practice, Research Studies Press, UK, 2000.
[2] F. Magalhães, A. Cunha. Explaining operational modal analysis with data from an arch bridge. Mech. Sys. Sig. Proc., 25 (5), pp. 1431–1450. 2011.
[3] P. L. Reu, D. P. Rohe, L. D. Jacobs, Comparison of DIC and LDV for practical vibration and modal measurements, Mech. Sys. Sig. Proc., 86(B), 2017, 2-16.
[4] W. Wang, JE. Mottershead. Adaptive moment descriptors for full-field strain and displacement measurements. J Strain Anal. Engng. Design. 48(1), pp.16-35. 2013.
[5] S. R. Ibrahim, E. C. Mikulcik. A method for direct identification of vibration parameters from the free response. Shock Vibn Bulletin, 47(4):183–98. 1977.
[6] D.M. Siringoringo, Y. Fujino. System identification of suspension bridge from ambient vibration response. Eng. Struct., 30 (2), pp. 462–477. 2008.
[7] B. Peeters, G. De Roeck. Referenced-based stochastic subspace identification for output-only modal analysis. Mech. Sys. Sig. Proc., 13(6), 855-878. 1999.
[8] R. Brincker, L. Zhang, P. Andersen. Modal identification from ambient responses using frequency domain decomposition, in Proceedings of the IMAC 18, International Modal Analysis Conference, San Antonio, USA, pp. 625-630. 2000.
[9] C. Devriendt, P. Guillaume. The use of transmissibility measurements in output-only modal analysis, Mech. Sys. Sig. Proc., 21 (7) 2689–2696. 2007.
[10] I. G. Araújo, J. E. Laier. Operational modal analysis approach based on multivariable transmissibility with different transferring outputs. J Sound and Vibration, 351, 90-105. 2015.
[11] B. Peeters, H. Van Der Auweraer. PolyMax: a revolution in operational modal analysis, in: Proceedings of the IOMAC, International Operational Modal Analysis Conference, Copenhagen, Denmark, pp. 13-24. 2005.
[12] K. V. Yuen, L. S. Katafygiotis. 2003. Bayesian fast fourier transform approach for modal updating using ambient data. Adv. Structural Engineering., 6(2), 2003, 81-95.
[13] S. K. Au. Fast Bayesian FFT Method for Ambient Modal Identification with Separated Modes. J. Eng. Mech., 137(3), pp. 214-226, 2011.
[14] W. Wang, J. E. Mottershead, C. Mares. Vibration mode shape recognition using image processing. J Sound Vibn., 326(3-5), pp.909-938. 2009.
[15] W. Wang, J. E. Mottershead, C. Mares. Mode-shape recognition and finite element model updating using the Zernike moment descriptor. Mech. Sys. Sig. Proc., 23(7), pp.2088-2112. 2009.
[16] W. Wang, J. E. Mottershead, A. Ihle, T. Siebert, H. R. Schubach. Finite element model updating from full-field vibration measurement using digital image correlation. J Sound Vibn., 330(8), pp.1599-1620. 2011.
[17] W. Wang, J.E. Mottershead, T. Siebert and A. Pipino, Frequency response functions of shape features from full-field vibration measurements using digital image correlation, Mech. Sys. Sig. Proc., 28, 2012, 333-347.